

PAPER • OPEN ACCESS

## Synthesis and characterization of secondary amine-functionalized silica for CO<sub>2</sub> capture

To cite this article: Abdul Rahman Abdul Rahim *et al* 2021 *IOP Conf. Ser.: Earth Environ. Sci.* **765** 012091

View the [article online](#) for updates and enhancements.

### You may also like

- [Enhancement of carbon dioxide adsorption performances by hydrazinolysis of poly\(n-vinylformamide\) grafted fibrous adsorbent](#)  
N A Zubair, M M Nasef, E C Abdullah *et al.*
- [A brief on tetraethylenepentamine \(TEPA\) functionalized-adsorbents in CO<sub>2</sub> capture application](#)  
K. W. Tan, A.H. Ruhaimi, C.N.C. Hitam *et al.*
- [Novel amine functionalized metal organic framework synthesis for enhanced carbon dioxide capture](#)  
Junaid Khan, Naseem Iqbal, Aisha Asghar *et al.*



The Electrochemical Society  
Advancing solid state & electrochemical science & technology

243rd ECS Meeting with SOFC-XVIII

**More than 50 symposia are available!**

Present your research and accelerate science

Boston, MA • May 28 – June 2, 2023

[Learn more and submit!](#)

# Synthesis and characterization of secondary amine-functionalized silica for CO<sub>2</sub> capture

Abdul Rahman Abdul Rahim<sup>1</sup>, Tay Tze Hao<sup>1</sup>, Ahmad Aizat Wan Azhari<sup>1</sup>,  
Norasikin Saman<sup>2</sup>, Hanapi Mat<sup>2</sup> and Khairiraihanna Johari<sup>1,3,\*</sup>

<sup>1</sup> Department of Chemical Engineering, Faculty of Engineering, Universiti Teknologi PETRONAS, 32610, Bandar Seri Iskandar, Perak, Malaysia.

<sup>2</sup> Advanced Materials and Processing Engineering Laboratory, School of Chemical and Energy Engineering, Faculty of Engineering, Universiti Teknologi Malaysia, 81310 UTM Skudai, Johor Bharu, Johor, Malaysia

<sup>3</sup> Centre of Contamination Control and Utilization (CenCoU), Department of Chemical Engineering, Universiti Teknologi PETRONAS, 32610 Seri Iskandar, Perak, Malaysia.

\*Email: khairiraihanna.j@utp.edu.my

**Abstract.** As one of commonly used technique for carbon dioxide (CO<sub>2</sub>) removal, amine-absorption also required high amounts of energy for adsorbent regeneration and problems of equipment corrosion during chemical holding may happened. Alternatively, amine-impregnated solid adsorbent received wide attention for CO<sub>2</sub> removal. However, there are limitations on the adsorbents' adsorption capacity and their hydrolytic stability. In this study, amine-functionalized silica (T-Si) adsorbent was synthesized via oil-in-water emulsion technique using centrimonium bromide (CTAB) as surfactant, ethanol as oil phase, and tetraethyl orthosilicate (TEOS) as silica precursor followed with impregnation with secondary amine (tetraethyl pentamine, TEPA). Results indicated that T-Si<sub>2</sub> adsorbent has a surface area of 10.7338 m<sup>2</sup>/g, presence of amine group (N-H) peaks in the FTIR spectra, and is thermally stable up to temperature of 170 °C. CO<sub>2</sub> adsorption study also shows that the T-Si also performed higher adsorption capacity (0.63 mmol/g) towards CO<sub>2</sub> compared to the blank Si adsorbent (0.33 mmol/g). The obtained experimental data show a good fitting into Sips adsorption isotherm which indicate a multilayer adsorption that happen on a heterogenous surface. The findings of this study show that the introduction of amine groups from TEPA offers improvement towards CO<sub>2</sub> capture due to the reaction with amine groups.

## 1. Introduction

Public concerns over the global warming and climate change have been widely reported due to the increasing of CO<sub>2</sub> concentration in the atmosphere. Major anthropogenic sources of CO<sub>2</sub> emission to environment are conventional fossil fuels such as coal, oil and natural gas combustions [1] for the purpose of electricity generation, transportation and industrial sector [2]. According to the Emission Database for Global Atmospheric Research [3], the atmospheric CO<sub>2</sub> level has increased to the high level of 400 ppm in May 2013 [4]. Due of these global concerns, strict regulations of CO<sub>2</sub> emission to the atmosphere have been imposed.



In the natural gas industry, CO<sub>2</sub> and other acid gases must be removed due to the presence of water, in which can form acids that corrode pipelines and other equipment [5]. Many efforts have been made to develop efficient CO<sub>2</sub> capture technologies such as cryogenic, membranes, adsorption and absorption [5–7]. Although all these approaches have been widely used to the separation of CO<sub>2</sub> from gas mixtures, however it have several drawbacks for post-combustion applications such as high energy consumption and high equipment corrosion rate, amine losses due to evaporation and thermal and chemical degradation of amines in the presence of oxygen [8, 9]. Therefore, an alternative technique was discovered for post combustion of CO<sub>2</sub> capture by adsorption [5], which offering potential energy savings with lower capital and operating cost [9].

The success of the adsorption process depends on the design of highly specific CO<sub>2</sub> solid adsorbent materials. Several solid adsorbents such as microporous organic polymers (MOPs), carbonaceous (graphene, activated carbon, carbon nanotubes), metal organic frameworks (MOFs), zeolites and ordered mesoporous silica have shown strong potential for CO<sub>2</sub> capture [10, 11]. It was reported that each adsorbent has a different physical and chemical properties, in which no ideal adsorbent is available yet due to various limitations related with either low adsorption capacity, slow kinetics, sensitivity to moisture, and high costs [12]. Ruffored et al. (2012) reported that the strength of the gas-solid interaction is determined by the characteristics if the adsorbent's surface chemistry and pores structures, as well as by the adsorbate's properties such as molecule size, polarizability and quadrupole moments [4]. Therefore, extensive studies are still being carried out to produce an adsorbent with robust performance in the presence of moisture and other contaminants that may be in the natural gas feed to the adsorption treating unit.

Discovery of ordered mesoporous silica materials such as MCM-41, MCM-48, SBA-12, SBA-15 and HMS have been widely employed for CO<sub>2</sub> capture in industrial gas separations [13]. Zhao et al. (1998) reported that these mesoporous silica materials facilitate rapid gas diffusion, however the affinity of CO<sub>2</sub> with silica surfaces is not as strong to the interaction of CO<sub>2</sub> with cationic sites of zeolites and MOFs [13]. Thus, several studies have been carried out to enhance the CO<sub>2</sub> capacity of mesoporous silica by grafting amine groups to the hydroxyl sites on the silica surface [5, 6, 14, 15]. The amine loading in CO<sub>2</sub> adsorption is believed to facilitate by chemical adsorption mechanism between surface silanol groups and aminosilane molecules [6, 13, 16, 17], in which produced amine modified porous silicas with high thermal stability, good water tolerance and high selectivity towards CO<sub>2</sub> [18]. In addition, several amine groups such as polyethyleneimine (PEI) [6], tetraethylenepentamine (TEPA) [17, 19], monoethanolamine (MEA) [20], 3-aminopropyltriethoxysilane (APTES) [6, 21, 22] have been performed in high adsorption capacity for CO<sub>2</sub>. Hence, the purpose of this research is to produce a hybrid silica adsorbent impregnated with secondary amine namely TEPA using soft templating method. Regarding this, its utilization as CO<sub>2</sub> adsorbent should be attractive than conventional adsorbents due to simple preparation process and easily functionalization with various functional groups that have high affinity towards CO<sub>2</sub>.

## 2. Methodology

### 2.1. Materials and chemicals

The chemicals that was used in this study such as centryltrimethylammonium bromide (CTAB, 99.9 %), tetraethylenepentamine (TEPA, 99.9 %) were purchased from Merck, Germany. Tetraethylethoxysilane (TEOS, 99.9%) were purchased from Sigma-Aldrich, Malaysia while ammonium hydroxide (NH<sub>4</sub>OH, 25.0%) and ethanol (C<sub>2</sub>H<sub>5</sub>OH, 99.5 %) were from Fisher Scientific. The deionized water used in this study were obtained from the laboratory.

### 2.2. Synthesis of blank silica adsorbent (B-Si)

The blank silica (B-Si) adsorbent was synthesized according to the method described by Maia et al. (2012) with some modifications [23]. Firstly, 0.25 g of CTAB was dissolved in 36 mL of water, followed

with addition of 0.25 mL of ammonia solution into the mixture to form Solution 1. Subsequently, Solution 1 was stirred using magnetic stirrer of 700 rpm for 30 minutes. In order to instigate the microemulsion, 18 mL of ethanol (Solution 2) was then added into Solution 1 and the mixture was stirred for another 30 minutes at 700 rpm. 2 mL of TEOS was then added into the mixture dropwise using a micropipette. Afterwards, the mixture was then continuously stirred using the magnetic stirrer of 700 rpm for 24 hours. The resultant precipitate was then filtered using vacuum filtration and were washed with deionized water. It was then dried in an oven at  $70 \pm 0.5$  °C for 24 hours. The dried final product was denoted as B-Si.

### 2.3. Synthesis of amine-functionalized silica adsorbent (T-Si)

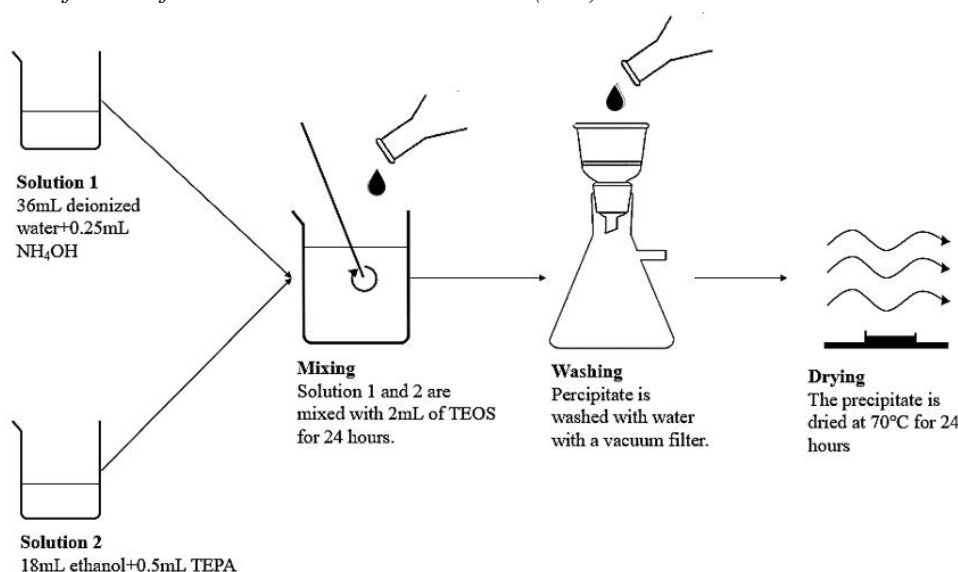


**Figure 1.** Synthesis of amine-functionalized silica adsorbent.

The amine-functionalized silica adsorbent were synthesized by employing the method use to synthesize the B-Si with the modifications of dissolving 0.05 g of TEPA in Solution 2 as shown in Figure 1. Afterwards, the mixture was then stirred on the magnetic stirrer of 700 rpm for 24 hours. The precipitate form was then filtered using the vacuum filtration and were washed with deionized water, followed by oven-drying at  $70 \pm 0.5$  °C for 24 hours. The final product is denoted as T-Si<sub>1</sub>. The steps to synthesis T-Si was illustrated in Figure 1. This method was repeated by increasing the content of TEPA to 0.1 g and 0.15 g as to examine the effect of different TEPA loading on CO<sub>2</sub> adsorption capacity. The synthesized adsorbent was denoted as T-Si<sub>1</sub>, T-Si<sub>2</sub> and T-Si<sub>3</sub> according to the respective TEPA cargo: 0.05g, 0.10g and 0.15g.

### 2.4. Characterization of adsorbents

The surface morphology of the synthesized adsorbents was observed with a Field Emission Scanning Electron Microscope (FESEM) VPFESM, Zeiss Supra55 VP and Transmission Electron Microscope (TEM), Zeiss Model Libra 200. The Fourier Transform Infrared (FTIR) Perkin Elmer Model 2000 spectrometer was used to determine the surface functional group of the adsorbent in the wavelength region of 4000 to 400  $\text{cm}^{-1}$ . The surface area and porosity characteristic of the adsorbents were measured by Nitrogen adsorption/desorption method using Micromeritics ASAP 2020. Thermogravimetric analysis (TGA) model of Perkin Elmer was used to measure the thermal stability of the synthesized adsorbents by heating it up from room temperature to 1000°C.

### 2.5. Measurement of CO<sub>2</sub> adsorption

The CO<sub>2</sub> adsorption performance of the synthesized adsorbents were measured using the BELSORP Mini II apparatus. The samples were degassed at 120°C for 2 hours in N<sub>2</sub> gas and then subjected to CO<sub>2</sub> adsorption for 2 hours at a pressure of 1 atm. The obtained CO<sub>2</sub> adsorption data were analysed using several adsorption isotherm models namely Langmuir, Freundlich and Sips isotherm model.

## 3. Results and discussions

### 3.1. Surface morphology

Figure 2 shows the morphology of the synthesized adsorbents as characterized by SEM and TEM. It was observed that nanospheres of approximately 500 nm were being synthesized via the oil-in-water microemulsion technique for both B-Si and T-Si<sub>2</sub>. The average diameter for both B-Si and T-Si<sub>2</sub> are also similar with adsorbent that has been synthesized by Teng [24]. However, the cracks observed in the synthesized adsorbents shows a solid inner body. This suggests that the synthesized adsorbents are solid nanospheres instead of hollow nanospheres. It could also be observed that functionalizing the synthesized adsorbents did not affect the morphology of the adsorbents as B-Si and T-Si<sub>2</sub> very similar. TEM imaging of the synthesized silica adsorbent (represented by the smaller rectangular image shows that the synthesized adsorbents are solid with no hollowed structured with particle size smaller than 600 nm. Similar with the SEM imaging in Figure 2, both blank and TEPA-functionalized silica adsorbent are very similar.

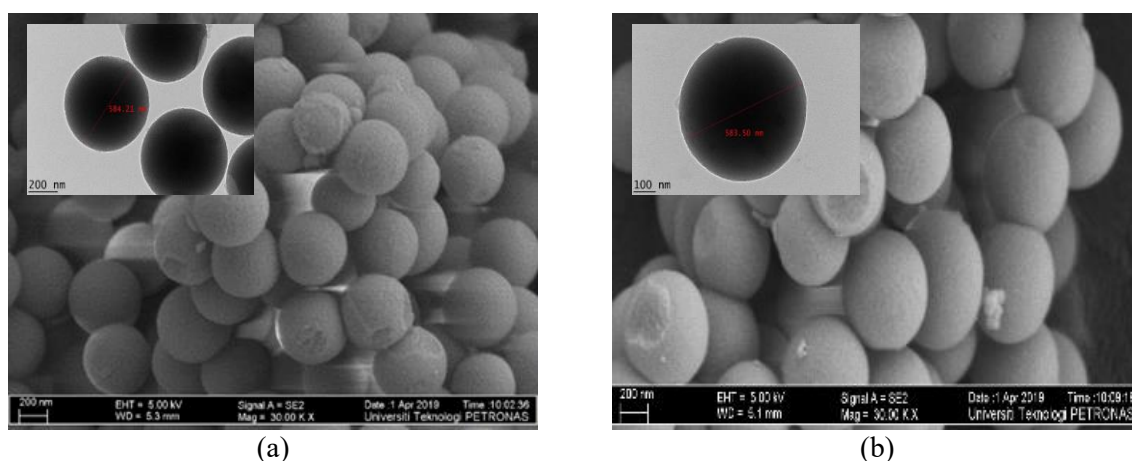


**Figure 2.** Surface morphologies images of silica adsorbents: a) B-Si and b) T-Si<sub>2</sub>

### 3.2. Surface properties

**Table 1.** Surface characteristic of the silica adsorbents

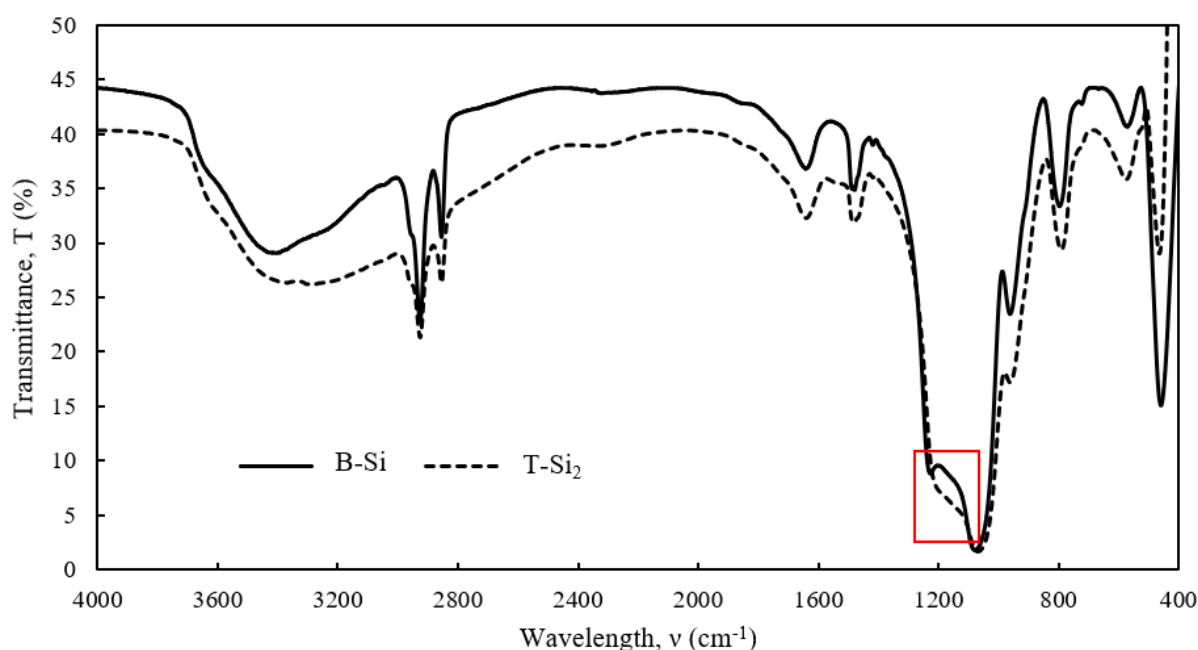
	BET surface area (m <sup>2</sup> /g)	Pore volume (cm <sup>3</sup> /g)	Pore size (nm)
B-Si	14.1517	0.0350	9.6928
T-Si <sub>2</sub>	10.7338	0.0227	8.5124

Table 1 shows the surface characteristics of the silica adsorbents such as surface area, pore volume and pore size. The surface area of B-Si is 14.157 m<sup>2</sup>/g which has a low surface area compared to the other reported surface area of silica adsorbent, 151 m<sup>2</sup>/g [25], 968 m<sup>2</sup>/g [24] and 187 m<sup>2</sup>/g [26]. This might suggest that the synthesized silica adsorbents, B-Si and T-Si<sub>2</sub> could be non-porous as shown in the FESEM results, represented in Figure 2. From Table 1, it could also be observed that T-Si<sub>2</sub> has a smaller pore volume, pore size and surface area as compared to B-Si. This could be due to the blockage of the

tetraethylenepentamine in the pores of the T-Si<sub>2</sub>. The blockage of cargo or functional groups onto the pores and surfaces of the silica pores have also been reported to be present by Palaniappalan et al. [25] and Mahmoodi et al. [26].

### 3.3. Surface functional group

Figure 3 describe the FTIR spectra of B-Si and T-Si<sub>2</sub>. The detailed FTIR functional group description are being described as in Table 2. According to Table 2, both B-Si and T-Si<sub>2</sub> share similar bending and stretching due to the chemicals used to synthesized them. However, B-Si and T-Si<sub>2</sub> have a difference at the wavelength region of 1130-1270 cm<sup>-1</sup> as of the highlighted box in Figure 3 as T-Si<sub>2</sub> has a slightly higher bending at that range as compared to B-Si. In the wavelength region of 3000 - 4000cm<sup>-1</sup>, it could be observed that T-Si<sub>2</sub> stretches more than B-Si. This indicates the presence of the N-H group in T-Si<sub>2</sub> in addition to the already present alcohol group which is present in both B-Si and T-Si<sub>2</sub>. Similar observation were reported by Azarshin et al. (2017), where functionalization of the silica adsorbents with amine functional groups resulted in peak formation at the reported wavelength [27].



**Figure 3.** FTIR spectra for B-Si and T-Si<sub>2</sub> adsorbents

**Table 2.** FTIR spectra of adsorbents

Functional group	B-Si (cm <sup>-1</sup> )	T-Si <sub>2</sub> (cm <sup>-1</sup> )
C-H bending (TEPA, TEOS, CTAB, ethanol)	700 – 900	700 – 900
SiO stretching (TEOS)	1062	1062
C-H stretching (TEPA, TEOS, CTAB, ethanol)	1479 – 1639	1479 – 1639
C-H stretching (TEPA, TEOS, CTAB, ethanol)	2854 – 2920	2854 – 2920
SiO bending (TEOS)	459	459
C-N stretching (TEPA)	N/A	1130-1270
O-H and N-H stretching (ethanol, TEPA, TEOS)	3000 – 4000	3000 – 4000

### 3.4. Thermal stability of the adsorbent

TGA characterization is used to measure the thermal stability of samples at different temperatures. Figure 4 depicts the TGA results for B-Si, T-Si<sub>1</sub>, T-Si<sub>2</sub>, T-Si<sub>3</sub>. From Figure 4, it could be observed that all the synthesized adsorbents start to thermally decompose at approximately 170°C. Beyond the temperature of 170°C, the synthesized adsorbents start to lose their weight by thermal decomposition. This low thermal composition temperature make B-Si and T-Si's to be suitable only for low temperature CO<sub>2</sub> adsorption of lower than 200°C [27].

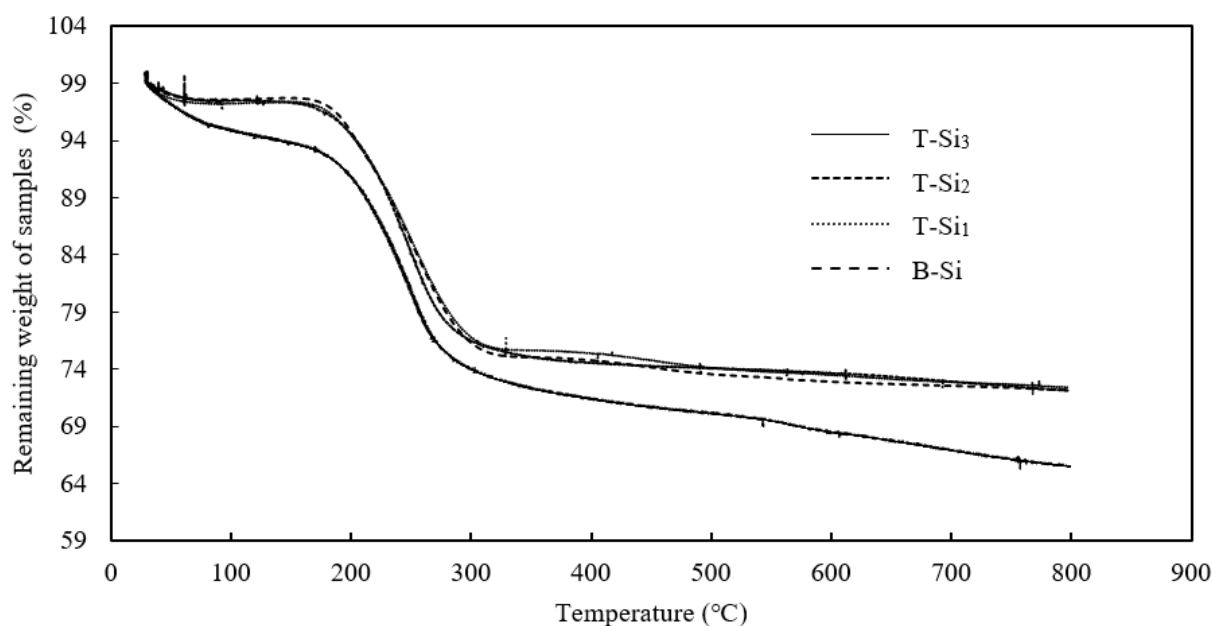


**Figure 4.** Thermogravimetric analysis of B-Si, T-Si<sub>1</sub>, T-Si<sub>2</sub>, and T-Si<sub>3</sub>

### 3.5. Effect of cargo loading

Figure 5 shows the B-Si behaviour on adsorption capacity as the relative pressure of CO<sub>2</sub> increases. It was observed that as the pressure of CO<sub>2</sub> increases, the adsorption capacity of the silica increased. The decrease in the adsorption capacity of silica adsorbent after reaching 0.22 mmol/g adsorption capacity for B-Si could be due to the weak interaction of CO<sub>2</sub> and the silica itself. The weak interaction disintegrates when the pressure is being increased which increases the stress exerted between the interaction. It could also be observed that as the loading of amine-functional group, TEPA increases, the adsorption capacity of CO<sub>2</sub> also increases. This could be explained by the presence of amine-functional group, TEPA on the T-Si's as TEPA has a high affinity to form chemical bond with CO<sub>2</sub> [20] to form carbamate ions while B-Si by itself only has a weak interaction with CO<sub>2</sub> [28, 29]. The higher the amount of TEPA on the B-Si, the higher the number of chemical bonds which could be made between CO<sub>2</sub> and the TEPA functional group.

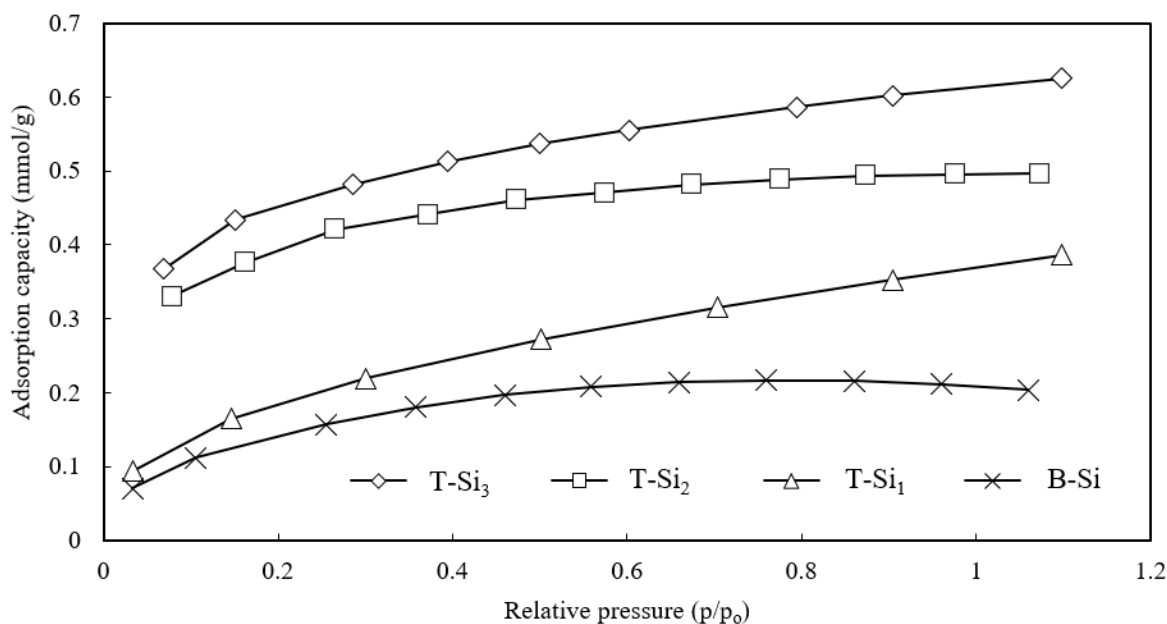


**Figure 5.** CO<sub>2</sub> adsorption capacity for silica adsorbent

**Table 3.** Adsorption isotherm parameters of CO<sub>2</sub> adsorption onto silica adsorbents.

		<b>B-Si</b>	<b>T-Si<sub>1</sub></b>	<b>T-Si<sub>2</sub></b>	<b>T-Si<sub>3</sub></b>
Langmuir	b (g/ms <sup>2</sup> )	4.76*10 <sup>-6</sup>	1.83*10 <sup>-6</sup>	7.07*10 <sup>-6</sup>	4.67*10 <sup>-6</sup>
	q <sub>m</sub> (mmol/g)	0.2331	0.4431	0.5251	0.6609
	R <sup>2</sup>	0.9921	0.9671	0.9963	0.9957
Freundlich	n	3.0602	2.4962	6.2909	5.2715
	K (L <sup>n</sup> m <sup>1-n</sup> /g)	0.0002	0.0002	0.0036	0.0030
	R <sup>2</sup>	0.9515	0.9986	0.9762	0.9991
Sips	n <sub>1</sub>	0.5903	0.3276	0.4855	0.2122
	K <sub>s</sub>	9.6191*10 <sup>-5</sup>	-0.0003	0.0006	0.0006
	q <sub>m</sub> (mmol/g)	0.3375	-0.8827	0.6361	4.5822
	R <sup>2</sup>	0.9962	0.9999	0.9978	0.9995

Meanwhile, Table 3 describes the constant values and correlations which have been calculated for the Langmuir and Freundlich and Sips adsorption isotherm models on the adsorption performance of B-Si and T-Si<sub>2</sub>. The experimental data exhibited that the Sips isotherm is best used to describe the adsorption behaviour of all the synthesized adsorbents due to the high correlation with all the adsorbents which is R<sup>2</sup>=0.99. Fitting into Sips adsorption isotherm indicated that the adsorption of the CO<sub>2</sub> by the adsorbents is multilayer adsorption process occurs on a heterogenous surface.

#### 4. Conclusions

Amine-functionalized silica adsorbent (T-Si) were successfully synthesized via an oil-in-water emulsion technique in a single stage polymerization step with average diameter of synthesized adsorbents of 500 nm. The T-Si which were synthesized had a lower surface area of 10.7338 m<sup>2</sup>/g while blank Si (B-Si) adsorbent has a higher surface area of 14.1517 m<sup>2</sup>/g. The results from FTIR have also confirmed the presence of amine-group on T-Si<sub>2</sub> compared to B-Si as T-Si<sub>2</sub> has stretch at 1130 – 1270 cm<sup>-1</sup> and further stretching at 3000 – 4000 cm<sup>-1</sup>. From the TGA results, it was also



confirmed that all the synthesized adsorbents start to thermally decompose at 170°C which makes it suitable only for low temperature CO<sub>2</sub> removal. From the current results of CO<sub>2</sub> adsorption, it could be concluded that the functionalization B-Si with TEPA would help to increase adsorption capacity from 0.22 mmol/g up to 0.65 mmol/g toward CO<sub>2</sub> in which the experimental data fitted the best into Sips adsorption isotherm model. This result has partially fulfilled the objective of the project by understanding the trend of CO<sub>2</sub> adsorption with TEPA loading and characteristics of the synthesized adsorbents.

## References

- [1] Leung DYCC, Caramanna G, Maroto-Valer MM 2014 *Renew Sustain Energy Rev* **39**: 426–443.
- [2] Rashidi NA, Yusup S 2016 *J CO<sub>2</sub> Util* **13**: 1–16.
- [3] Vogel C, Pendergrass W, White J. *National Oceanic and Atmospheric Administration*.
- [4] Rufford TE, Smart S, Watson GCY, et al. 2012 *J Pet Sci Eng* **94–95**: 123–154.
- [5] Vilarrasa-Garcia E, Moya EMO, Cecilia JA, et al. 2015 *Microporous Mesoporous Mater* **209**: 172–183.
- [6] Yu CH, Huang CH, Tan CS 2012 *Aerosol Air Qual Res* **12**: 745–769.
- [7] Villegas MR, Baeza A, Vallet-Regí M 2015 *ACS Appl Mater Interfaces* **7**: 24075–24081.
- [8] Ammendola P, Raganati F, Chirone R 2017 *Chem Eng J* 2017; **322**: 302–313.
- [9] Younas M, Sohail M, Leong LK, et al. 2016 *Int J Environ Sci Technol Vol* **13**: 1839–1860.
- [10] Creamer AE, Gao B 2016 *Environ Sci Technol* **50**: 7276–7289.
- [11] Hornbostel MD, Bao J, Krishnan G, et al. 2013 *Carbon N Y* **56**: 77–85.
- [12] Ünveren EE, Monkul BÖ, Sarıođlan Ş, et al. 2017 *Petroleum* **3**: 37–50.
- [13] Zhao D, Feng J, Huo Q, et al. 1998 *Science (80- )* **279**: 548–552.
- [14] Araki S, Doi H, Sano Y, et al. 2009 *J Colloid Interface Sci* **339**: 382–389.
- [15] Vilarrasa-García E, Cecilia JA, Santos SML, et al. 2014 *Microporous Mesoporous Mater* **187**: 125–134.
- [16] Wang X, Guo Q, Kong T 2015 *Chem Eng J* **273**: 472–480.
- [17] Siriwardane R V., Shen MS, Fisher EP, et al. 2001 *Energy and Fuels* **15**: 279–284.
- [18] Zhang G, Zhao P, Xu Y 2017 *J Ind Eng Chem* **54**: 59–68.
- [19] Chatti R, Bansawal AK, Thote JA, et al. 2009 *Microporous Mesoporous Mater* **121**: 84–89.
- [20] Kishor R, Ghoshal AK 2015 *Chem Eng J* **262**: 882–890.
- [21] Quang DV, Hatton TA, Abu-Zahra MRM 2016 *Ind Eng Chem Res* **55**: 7842–7852.
- [22] Zhang Y, Hsu BYW, Ren C, et al. 2015 *Chem Soc Rev* **44**: 315–335.
- [23] Maia F, Tedim J, Lisenkov AD, et al. 2012 *Nanoscale* **4**: 1287–1298.
- [24] Teng Z, Han Y, Li J, et al. 2010 *Microporous Mesoporous Mater* **127**: 67–72.
- [25] Palaniappan T, Saman N, Mat H, et al. 2017 Synthesis and characterization of sulfur-functionalized silica nanocapsules as mercury adsorbents. In: *AIP Conference Proceedings*. 2017. DOI: <https://aip.scitation.org/doi/abs/10.1063/1.5010455>.
- [26] Mahmoodi NM, Khorramfar S, Najafi F 2011 *Desalination* **279**: 61–68.
- [27] Azarshin S, Moghadasi J, A Aboosadi Z 2017 *Energy Explor Exploit* **35**: 685–697.
- [28] Qi G, Wang Y, Estevez L, et al. 2011 *Energy Environ Sci* **4**: 444–452.
- [29] Ramli A, Ahmed S, Yusup S 2014 *Chem Eng Trans* **39**: 271–276.

## Acknowledgments

Financial support from Yayasan Universiti Teknologi PETRONAS Research Grant (Project No: 015LCO-051) are gratefully acknowledge.